Asian Journal of Chemistry; Vol. 34, No. 11 (2022), 2984-2988

ASIAN JOURNAL OF CHEMISTRY

https://doi.org/10.14233/ajchem.2022.23993

UV Light Photo-Degradation of Rhodamine B and Methylene Blue Dyes using Gd_2O_3 Nanoparticles

THANINKI LEENA VINOLIA[1,2], ARPUTHARAJ SAMSON NESARAJ[1,3,*] and MANASAI ARUNKUMAR[1]

[1]Department of Applied Chemistry, Karunya Institute of Technology and Sciences (Deemed to be University), Coimbatore-641114, India
[2]Department of Chemistry, CMR Technical Campus, Kandlakoya, Hyderabad-501401, India
[3]Department of Chemistry, School of Advanced Sciences, Kalasalingam Academy of Research and Education (Deemed to be University), Krishnankoil-626126, India

*Corresponding author: E-mail: samson@klu.ac.in

Received: 11 July 2022; *Accepted*: 3 September 2022; *Published online*: 19 October 2022; AJC-21017

The detoxification of numerous harmful and toxic contaminants as well as water treatment is done successfully by photocatalytic oxidation. The potential uses of metal oxide, which are defined as charge carriers in electronic structure, enhance its light-absorbing qualities when exposed to a particular type of radiation and enable its use as a photocatalyst. Metal oxide nanoparticles, as photocatalyst, are used in waste-water treatment in removing pollutants and the degradation of dyes, thus can render water reusable. In the current investigation, XRD and SEM studies were utilized to analyze the rare earth Gd_2O_3 nanoparticles that were synthesized using the chemical precipitation approach. Additionally, degradation of Rhodamine B and methylene blue in aqueous solution under UV light was used to assess the photocatalytic activity. The results indicated that the synthesized Gd_2O_3 material exhibits good photocatalytic activity.

Keywords: Gd_2O_3 nanoparticles, Chemical precipitation method, Photocatalytic degradation, Rhodamine B, Methylene blue.

INTRODUCTION

Maintaining the ecological balance is crucial for a healthy ecosystem and one aspect of this is reducing the amount of hazardous chemicals in the environment. In order to create smart materials that are effective in sensing and concurrently remove dangerous chemical contaminants from the environment, metal oxide nanostructures are essential. Metal oxide materials that have been reduced in size to the nanoscale have features that distinguish them from the bulk and these nanoparticles behave like lone atoms and molecules [1]. Nanostructures of metal oxides and semiconductors are unavoidable materials because of their unique properties and prospective uses. Their exceptional qualities are caused by their significant particulate characteristics. Metal oxides are potent decolourizing agents that are used in the efficient photocatalytic destruction of organic contaminants in wastewater effluents. Because of ultrafine nature of metal oxide ceramic nanoparticles, they can exhibit better electrochemical liquid/surface interactions in the identification of various hazardous chemicals [2].

When UV light is present, a photocatalyst uses the catalyst to accelerate chemical reactions. Widespread use of photocatalysis results in the removal of toxic substances, the deactivation and destruction of all waterborne bacteria, as well as the elimination of organic pollutants as carbon dioxide and water. The appropriate band gap, proper shape, large surface area, stability and reusability of the photocatalytic system are important characteristics [3,4]. Therefore, the term "photocatalysis" refers to the oxidation and reduction processes carried out on the surface of the photocatalyst material by valence band (VB) particles like holes and conduction band (CB) particles like electrons produced by the absorption of UV-vis light radiation. Metal oxide nanomaterials cause the excitation of an electron from VB to CB giving rise to an electron-hole pair upon exposure to a sufficient wavelength, either larger or equal to band gap energy. In the presence of oxygen and water, the electron in the CB is taken up by oxygen, resulting in the super oxide radical anion and water is oxidized at the oxidation site, producing the OH^- radical. These photogenerated species can decrease and/or oxidize a chemical that has been adsorbed on the surface of the photocatalyst. The process of degradation may begin when the hole interacts with the dye molecule and takes an electron from it [5-9].

The oxidation-reduction process involved in the mechanism of photocatalysis can be represented in Fig. 1. By using metal oxides including TiO_2, ZnO, SnO_2 and CeO_2, heterogeneous photocatalysis has demonstrated its effectiveness in converting a variety of pollutants into biodegradable molecules, which can then be mineralized into the innocuous gases CO_2 and H_2O [10-13]. Due to the activation of holes and electrons by visible light, a direct band gap semiconductor or an inorganic compound like cadmium sulphide has received interest for the photocatalytic destruction of organic contaminants [14,15].

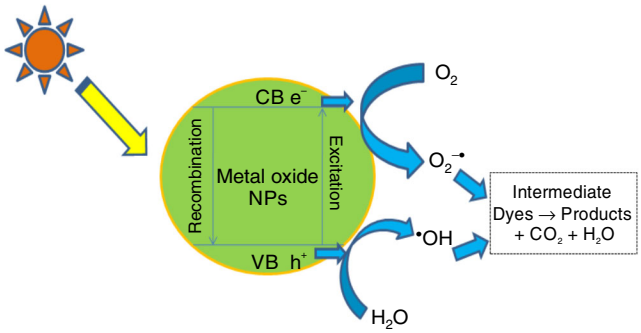

Fig. 1. Mechanism of photocatalysis

Now-a-days, lanthanide oxide like Gd_2O_3 is proposed to be used in many applications. The 4*f*-orbitals of gadolinium, which have an effective ionic radius of 0.0938 nm (Gd^{3+}), only contain seven electrons [16]. The inorganic compound Gd_2O_3, sometimes known as gadolinia and is the most accessible forms of Gd_2O_3, moreover its derivatives have potential as MRI contrast agents [17]. When exposed to visible light, $Gd_2O_3/BiVO_4$ photocatalysts showed increased photodegradation compared to pure $BiVO_4$ for the degradation of methyl orange [18].

The significant pollutants from the paper, dye and textile industries are the synthetic colours, which generally includes methyl orange, methylene blue or methyl green, which have a negative impact on the environment. After the process, 10-15% of these colours are liberated [19]. The organic dyes present in water may become carcinogenic when they decompose [20]. Hence, suitable methodologies are required to remove these substances carefully without affecting the environment [21]. Despite of several conventional methods, photodegradation has been proposed as an efficient method for the removal of dyes.

Among various dyes, Rhodamine B and methylene blue are also disposed into nearby water bodies by textile and paper industries which contribute towards water pollution causing threat to aquatic organisms and health risks as well. Therefore, there is an immense need to treat/remove these coloured effluents from water. Rhodamine B is an amphoteric dye and represent xanthene dyes, is being listed as basic due to overall positive charge. It gives a characteristic absorbance at ~553 nm [22]. A cationic dye widely used in the textile industry is methylene blue. It is an odourless, dark green powder at ambient temperature that when dissolved in water turns blue. At 653 nm, it has a recognizable spectrophotometric absorbance. The development of novel, intriguing materials for dye removal has been the subject of extensive research. Rhodamine B and methylene blue dyes are extremely bad for the ecology and endanger the environment. Numerous studies have examined the mechanisms underlying Rhodamine B degradation in recent years [23,24], with N-de-ethylation of Rhodamine B identified as the primary process [25].

In present study, chemical precipitation was used to create nanosized Gd_2O_3 particles, which were then examined using SEM and XRD techniques. Two dyes *viz*. Rhodamine B and methylene blue dyes were used as a model for the photodegradation of organic contaminants from industrial effluents and the synthesized Gd_2O_3 nanoparticles were used as photocatalyst for this experiment.

EXPERIMENTAL

The materials required for the synthesis of Gd_2O_3 nanoparticles were used as such without any further purification. The chemicals *viz*. gadolinium nitrate (99% pure grade from Thermo Fisher Scientific, India), sodium hydroxide (97% purity, Merck, India), Rhodamine B (Practical grade, HI media, India), Methylene blue (Fisher Scientific, India) and ethanol (99% pure, China make). All the reagents were prepared in ultrapure water.

Synthesis of Gd_2O_3 nanoparticles: Gd_2O_3 nanoparticles were synthesized by chemical precipitation method. In brief, gadolinium nitrate and NaOH solutions with appropriate concentrations were prepared using double distilled water. These solutions were thoroughly mixed and then stirred magnetically for 2 h at room temperature. The resulting white precipitate was filtered under suction, rinsed with a 9:1 water-ethanol solution and then dried for an extended period of time in a hot air oven at 60 ºC. The dry precipitate was ground well in a mortar and pestle and then calcined for 2 h at each of 150, 300, 450 and 600 ºC.

Structural characterization of Gd_2O_3 nanoparticles: By employing Cu$K\alpha$ = 0.154059 nm in the presence of a nickel filter at 40 kV at 30 mA power on a Shimadzu XRD6000, the crystal structure of the synthesized Gd_2O_3 nanoparticles was identified. The sample's morphology was examined using a scanning electron microscope (SEM JEOL JSM-6610). Shimadzu 1800 UV spectrophotometer was used to measure the photocatalytic behaviour of the sample between 200 and 800 nm.

Photocatalytic activity: As water pollutants, Rhodamine B and methylene blue dyes were utilized to examine the photocatalytic behaviour of gadolinium oxide nanoparticles. The technique includes exposing the Gd_2O_3 photocatalyst to light, which produces an electron-hole pair. By absorbing electrons, oxygen produces the extremely reactive intermediates H_2O_2 and an oxide radical anion. These react to produce hydroxyl radicals ($OH^{\bullet}$), which have a strong oxidizing effect and cause the advanced oxidation process (AOP) and results in the degradation of the organic dye pollutions [26-28]. It can be represented as below (eqns. 1-5),

$$Gd_2O_3 + h\nu \longrightarrow Gd_2O_3(h^+) + e^- \quad (1)$$

$$e^- + O_2 \longrightarrow O_2^- \quad (2)$$

$$e^- + O_2 + 2H^+ \longrightarrow H_2O_2 \quad (3)$$

$$H_2O_2 + O_2^- \longrightarrow OH^\bullet + OH^- + O_2 \quad (4)$$

$$OH^\bullet + \text{Dye} \longrightarrow CO_2 + H_2O \text{ (Degradation products)} \quad (5)$$

To evaluate the process of degradation of the above dyes, 0.05 g of Gd_2O_3 nanoparticles as photocatalyst was dispersed in 50 mL of an aqueous solution of Rhodamine B dye (10^{-5} M). This solution was then taken in a Pyrex photoreactor consisting of 11 W-UV light source and mixed well in a magnetic stirrer in dark for about 0.5 h to attain the adsorption-desorption equilibrium of the dye solution on the photocatalyst sample surface. Then ~ 3 mL of solution was removed to observe the UV-visible absorption spectrum at 553 nm [22].

The solution was then taken out in aliquots of 3 mL every 20 min as needed. In order to determine the % degradation, the UV absorption spectra of the collected samples were taken. The degradation of methylene blue was investigated using the same process. The following formula was used to compute the percentage of dye degradation (eqn. 6) [29]:

$$\text{Dye degradation (\%)} = \frac{C_o - C_t}{C_o} \times 100 \quad (6)$$

where, C_o is the initial absorption of the dye solution and C_t is the absorption at a particular time (t).

RESULTS AND DISCUSSION

XRD studies: The synthesized Gd_2O_3 nanoparticles by chemical precipitation method were characterized by X-ray diffraction studies. Fig. 2 shows the X-ray diffraction pattern of the synthesized Gd_2O_3 nanoparticles. From the XRD data, the crystal structure was found to be cubic crystalline structure [30,31] and the diffraction peaks obtained were very sharp and intense as well with their 2θ = 20.4800º, 28.9049º, 33.4431º, 47.8643º, 56.7387º, 57.2405º, 59.2000º, 60.7207º, 68.5575º, 76.5337º, 78.0913º and 79.1784º that correspond to (2 1 1), (2 2 2), (4 0 0), (4 4 0), (6 2 2), (1 3 6), (4 4 4), (5 4 3), (1 5 6), (6 6 2), (7 5 2) and (0 4 8) planes, respectively. The average crystallite size involves using the high intensity peaks.

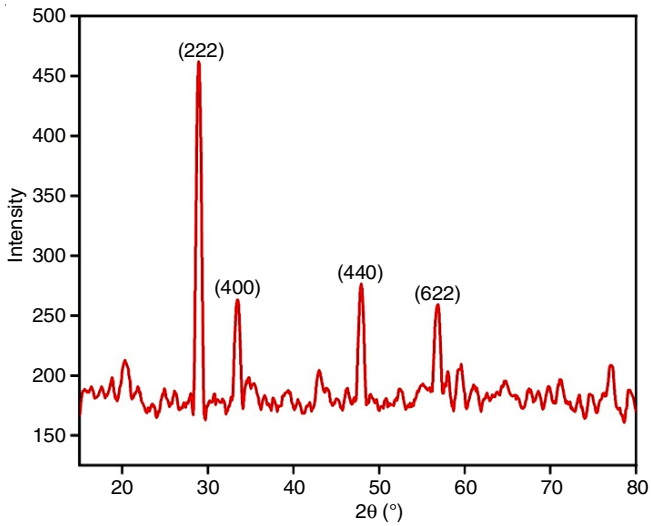

Fig. 2. XRD pattern obtained on Gd_2O_3 nanoparticles

In Fig. 2, the hkl values of high intensity peaks alone were shown. The JCPDS data with card no. 88-2165 and these results are well indexed and agreed well [32]. The crystallite size and theoretical density of the materials were calculated as per the standard procedure [33]. The crystallographic parameters obtained for pure Gd_2O_3 nanoparticles are given in Table-1.

SEM studies: The morphological images of the synthesized Gd_2O_3 nanoparticles at different magnifications are shown in Fig. 3. The particles' grain size was found to be in the nano-range.

Photocatalytic degradation studies: Rhodamine B and methylene blue dyes were taken as model contaminants from textile and paper industries. The photocatalytic degradation of these two organic dyes was studied by pure Gd_2O_3 nanoparticles (as photocatalyst) in presence of UV light source. The synthesized Gd_2O_3 nanoparticles, as metal oxide photocatalyst was first used in the degradation process of Rhodamine B and the same photocatalyst was further subjected to methylene blue degradation under UV light illumination.

TABLE-1
CRYSTALLOGRAPHIC PARAMETERS OBTAINED ON PARENT Gd_2O_3 NANOPARTICLES

Sample	Crystal structure	Unit cell parameter (Å)	Unit cell volume (Å^3)	Crystallite size (nm)	Theoretical density (g cm^{-3})
Gd_2O_3 JCPDS No.88-2165	Cubic (B.C.)	10.79	1256.22	–	7.667
Synthesized pure Gd_2O_3 nanoparticle	Cubic (B.C.)	10.81	1263.97	26.65	7.618

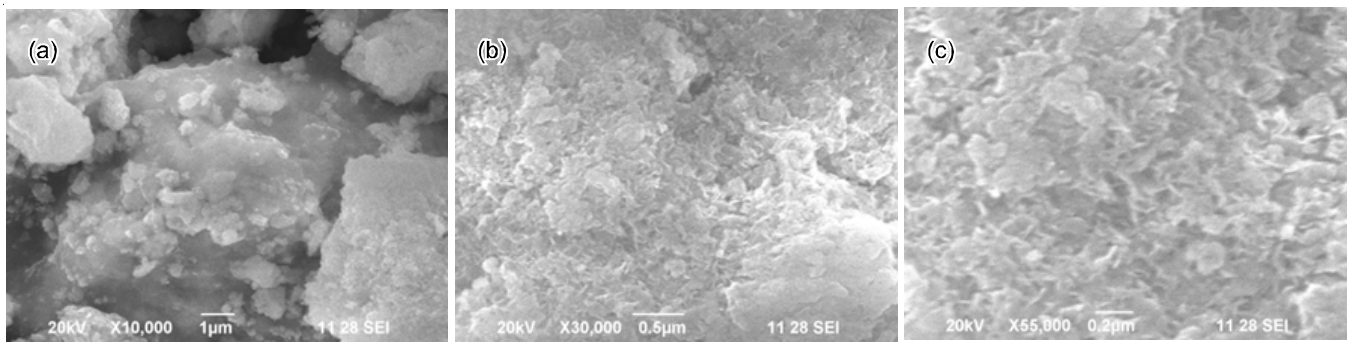

Fig. 3. SEM images of Gd_2O_3 nanoparticles in different magnifications (a) 10000x, (b) 30000x, (c) 55000x

The aqueous solutions of the dye stuff in presence of the prepared Gd_2O_3 photocatalyst was irradiated with UV light and the UV spectra of the degradation process was recorded at the regular time intervals of 0, 20, 40, 60 and 80 min, respectively. The absorption peak was centered at 553 nm for Rhodamine B and 662 nm for methylene blue [34] and different degradation patterns were seen for the synthesized photocatalyst. From the UV-spectral analysis, Rhodamine B and methylene blue dyes exhibit the absorption maximum peaks at 553 and 662 nm, respectively [22]. It was also clear that as the time of irradiation increases, the intensity of the peak decreases at their absorption maxima in both the photocatalytic degradation of dyes (Fig. 4). This can be attributed to the photodegradation of dyes by Gd_2O_3 photocatalyst in presence of UV light.

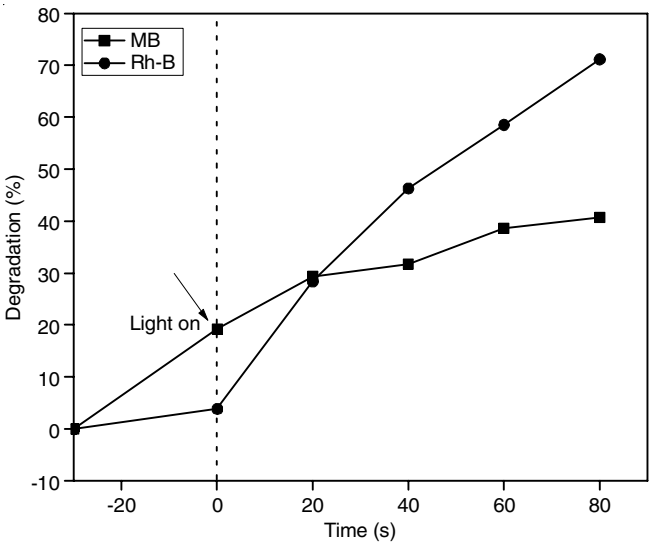

Fig. 4. Time-dependent photodegradation of Rhodamine B (Rh-B) and methylene blue (MB) using Gd_2O_3 photocatalyst on UV irradiation

Figs. 5 and 6 show the photodegradation of Rhodamine B and methylene blue in presence of pure Gd_2O_3 photocatalyst. The elimination of Rhodamine B by Gd_2O_3 photocatalyst was found to increase slowly and reaches a degradation of 71% at 80 min where 43% degradation in presence of Nb_2O_3 was reported [22] in the previous study. In general, degradation of methylene blue increase with increase of UV irradiation [35, 36]. Thus, in case of methylene blue dye, the percentage degradation has shown a gradual increase of 40% degradation at 80 min but found no significant increase in degradation further even on prolonged irradiation time. Further, a considerable rise in the degradation of Rhodamine B could be seen on prolonged irradiation time and thus at 120 min, Gd_2O_3 have shown 74.98 % degradation on Rhodamine B dye. The low percentage degradation results of methylene blue can be attributed to several factors that depend on the nature the catalyst, source of light used and also on the structure and the concentration of the dyes as well.

The low degradation percentage of methylene blue can also be attributed to low absorption capacity of light photon by the dye resulting in less availability of photons for hydroxyl

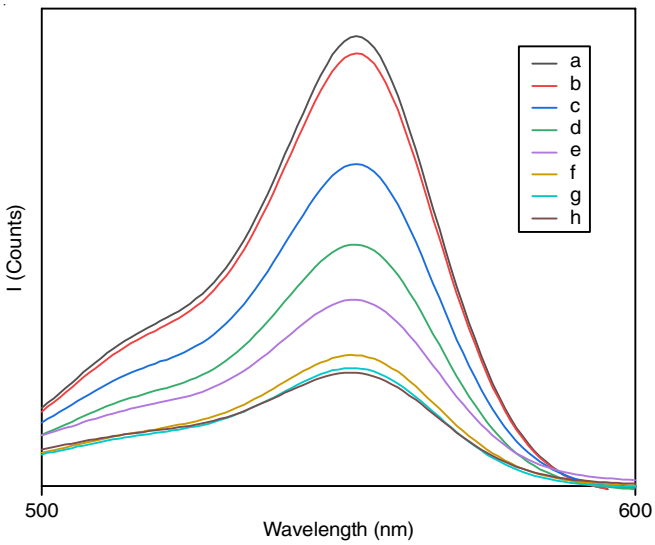

Fig. 5. Photodegradation spectrum of Rhodamine B obtained on pure Gd_2O_3 nanoparticles (a) At initial stage, (b) After 0 min, (c) After 20 min, (d) After 40 min, (e) After 60 min, (f) After 80 min, (g) After 100 min and (h) After 120 min

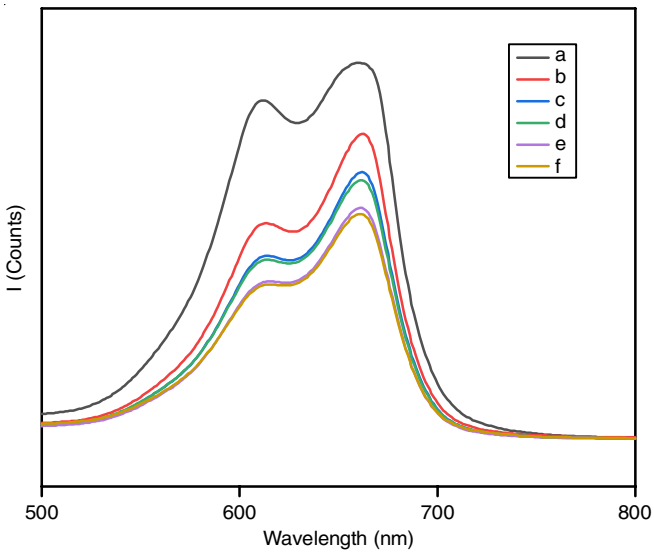

Fig. 6. Photodegradation spectrum of Methylene blue obtained on pure Gd_2O_3 nanoparticles (a) At initial stage, (b) After 0 min, (c) After 20 min, (d) After 40 min, (e) After 60 min and (f) After 80 min

radical generation. Their life time of hydroxyl radical is very short [37]. Moreover, the absorbance range of the dyes may sometimes lead to inhibition of holes/oxide radicals' production that are incapable of interacting with the photocatalyst [22]. It has also been reported that in such cases the photon may not reach the surface of the photocatalyst leading to decreased photodegradation efficiency [38-39]. The adsorption of dye molecules over the surface of Gd_2O_3 photocatlyst material is an important step during the photocatalytic reaction. The degradation efficiency can be enhanced by incorporating a dopant [40], increasing the concentration of the photocatalyst, longer irradiation period and also altering the pH values.

Conclusion

The present work dealt with the synthesis of Gd_2O_3 nanoparticles by chemical precipitation method. The synthesized

particles were calcined at different temperatures upto 600 ºC. The crystallographic structure and the morphological characteristics of the material were studied by XRD and SEM analysis. The synthesized material can effectively act as photocatalyst in the degradation of Rhodamine B and methylene blue, which are the major water pollutants from industrial effluents.

ACKNOWLEDGEMENTS

The authors thank Karunya Institute of Technology and Sciences (KITS) for providing necessary instrumental facilities to complete this work successfully.

CONFLICT OF INTEREST

The authors declare that there is no conflict of interests regarding the publication of this article.

REFERENCES

1. Y.M. Lin, S.B. Cronin, O. Rabin, J.Y. Ying and M.S. Dresselhaus, *Appl. Phys. Lett.*, **79**, 677 (2001); https://doi.org/10.1063/1.1385800
2. M.M. Rahman, G. Gruner, M.S. Al-Ghamdi, M.A. Daous, S.B. Khan and A.M. Asiri, *Chem. Cent. J.*, **7**, 60 (2013); https://doi.org/10.1186/1752-153X-7-60
3. E. Pelizzetti and C. Minero, *Comments Inorg. Chem.*, **15**, 297 (1994); https://doi.org/10.1080/02603599408035846
4. M.R. Hoffmann, S.T. Martin, W. Choi and D.W. Bahnemann, *Chem. Rev.*, **95**, 69 (1995); https://doi.org/10.1021/cr00033a004
5. N. Kislov, J. Lahiri, H. Verma, D Y. Goswami, E. Stefanakos and M. Batzill, *Langmuir*, **25**, 3310 (2019); https://doi.org/10.1021/la803845f
6. H. Zhu, R. Jiang, Y. Fu, Y. Guan, J. Yao, L. Xiao and G. Zeng, *Desalination*, **286**, 41 (2012); https://doi.org/10.1016/j.desal.2011.10.036
7. S. Baruah, M. Jaisai, R. Imani, M.M. Nazhad and J. Dutta, *Sci. Technol. Adv. Mater.*, **11**, 055002 (2010); https://doi.org/10.1088/1468-6996/11/5/055002
8. M. Nirmala, M.G. Nair, K. Rekha and A. Anukalini, *African J. Basic Appl. Sci.*, **2**, 161 (2010).
9. M. Qamar and M. Muneer, *Desalination*, **249**, 535 (2009); https://doi.org/10.1016/j.desal.2009.01.022
10. H. Chen, C.E. Nanayakkara and V.H. Grassian, *Chem. Rev.*, **112**, 5919 (2012); https://doi.org/10.1021/cr3002092
11. S.A. Ansari, M.M. Khan, S. Kalathil, A. Nisar, J. Lee and M.H. Cho, *Nanoscale*, **5**, 9238 (2013); https://doi.org/10.1039/c3nr02678g
12. H. Wang and A.L. Rogach, *Chem. Mater.*, **26**, 123 (2014); https://doi.org/10.1021/cm4018248
13. C. Sun, H. Li and L. Chen, *Energy Environ. Sci.*, **5**, 8475 (2012); https://doi.org/10.1039/c2ee22310d
14. Y. Yang, H. Yu, D. York, Q. Cui and M. Elstner, *J. Phys. Chem. C*, **111**, 10861 (2007); https://doi.org/10.1021/jp074167r
15. L. Li, Z. Lou and G. Shen, *ACS Appl. Mater. Interfaces*, **7**, 23507 (2015); https://doi.org/10.1021/acsami.5b06070
16. D. Wu, C. Li, D. Zhang, L. Wang, X. Zhang, Z. Shi and Q. Lin, *J. Rare Earths*, **37**, 845 (2019); https://doi.org/10.1016/j.jre.2018.10.011
17. N. Sakai, L. Zhu, A. Kurokawa, H. Takeuchi, S. Yano, T. Yanoh, N. Wada, S. Taira, Y. Hosokai, A. Usui, Y. Machida, H. Saito and Y. Ichiyanagi, *J. Phys. Conf. Ser.*, **352**, 012008 (2012); https://doi.org/10.1088/1742-6596/352/1/012008
18. M.M. Abdullah, M.M. Rahman, M. Faisal, S.B. Khan, P. Singh, M.A. Rub, N. Azum, A. Khan, A.A.P. Khan and M. Hasmuddin, *J. Colloid Sci. Biotechnol.*, **2**, 322 (2013); https://doi.org/10.1166/jcsb.2013.1069
19. Y. Aldegs, M. Elbarghouthi, A. Elsheikh and G. Walker, *Dyes Pigm.*, **77**, 16 (2008); https://doi.org/10.1016/j.dyepig.2007.03.001
20. C. Zaharia, D. Suteu, A. Muresan, R. Muresan and A. Popescu, *Environ. Eng. Manag. J.*, **8**, 1359 (2009); https://doi.org/10.30638/eemj.2009.199
21. S. Papic, N. Koprivanac, A. Bozic and A. Metes, *Dyes Pigm.*, **62**, 291 (2004); https://doi.org/10.1016/S0143-7208(03)00148-7
22. F. Hashemzadeh, R. Rahimi and A. Ghaffarinejad, *Int. J. Appl. Chem. Sci. Res.*, **1**, 95 (2013).
23. M.C. Cotto, T. Campo, E. Elizalde, A. Gomez, C. Morant and F.M. Marquez, *Am. Chem. Sci. J.*, **3**, 178 (2013); https://doi.org/10.9734/ACSJ/2013/2712
24. S. Rajalakshmi, S. Pitchaimuthu, N. Kannan and P. Velusamy, *Appl. Water Sci.*, **7**, 115 (2017); https://doi.org/10.1007/s13201-014-0223-5
25. A.A. Al-Kahtani, *J. Biomater. Nanobiotechnol.*, **8**, 66 (2017); https://doi.org/10.4236/jbnb.2017.81005
26. R.S. Ganesh, S.K. Sharma, E. Durgadevi, M. Navaneethan, H.S. Binitha, S. Ponnusamy, C. Muthamizhchelvan, Y. Hayakawa and D.Y. Kim, *Superlattices Microstruct.*, **104**, 247 (2017); https://doi.org/10.1016/j.spmi.2017.02.029
27. Y.Y. Lu, Y.Y. Zhang, J. Zhang, Y. Shi, Z. Li, Z.C. Feng and C. Li, *Appl. Surf. Sci.*, **370**, 312 (2016); https://doi.org/10.1016/j.apsusc.2016.02.170
28. M. Saranya, R. Ramachandran, E.J.J. Samuel, S.K. Jeong and A.N. Grace, *Powder Technol.*, **279**, 209 (2015); https://doi.org/10.1016/j.powtec.2015.03.041
29. Amita, Diksha and P.S. Rana, *AIP Conf. Proc.*, **2115**, 030109 (2019); https://doi.org/10.1063/1.5112948
30. G.K. Das, B.C. Heng, S.-C. Ng, T. White, J.S.C. Loo, L. D'Silva, P. Padmanabhan, K.K. Bhakoo, S.T. Selvan and T.T.Y. Tan, *Langmuir*, **26**, 8959 (2010); https://doi.org/10.1021/la904751q
31. V. Bedekar, D.P. Dutta, M. Mohapatra, S.G. Godbole, R. Ghildiyal and A.K. Tyagi, *Nanotechnology*, **20**, 125707 (2009); https://doi.org/10.1088/0957-4484/20/12/125707
32. D. Raiser and J.P. Deville, *J. Electron Spectrosc. Rel. Phenomena*, **57**, 91 (1991).
33. T.L. Vinolia and A.S. Nesaraj, *Integr. Ferroelectr.*, **221**, 186 (2021); https://doi.org/10.1080/10584587.2021.1965844
34. M. Sun, D. Li, Y. Chen, W. Chen, W. Li, Y. He and X. Fu, *J. Phys. Chem. C*, **113**, 13825 (2009); https://doi.org/10.1021/jp903355a
35. S.V. Elangovan, V. Chandramohan, N. Sivakumar and T.S. Senthil, *Superlattices Microstruct.*, **85**, 901 (2015); https://doi.org/10.1016/j.spmi.2015.07.004
36. S.K. Kansal, M. Singh and D. Sud, *J. Hazard. Mater.*, **141**, 581 (2007); https://doi.org/10.1016/j.jhazmat.2006.07.035
37. E.J. Land and M. Ebert, *Trans. Faraday Soc.*, **63**, 1181 (1967); https://doi.org/10.1039/tf9676301181
38. A.R. Khataee, M.N. Pons and O. Zahraa, *J. Hazard. Mater.*, **168**, 451 (2009); https://doi.org/10.1016/j.jhazmat.2009.02.052
39. N. Daneshvar, A. Aleboyeh and A.R. Khataee, *Chemosphere*, **59**, 761 (2005); https://doi.org/10.1016/j.chemosphere.2004.11.012
40. A. Barrera, F. Tzompantzi, J. Campa-Molina, J.E. Casillas, R. Pérez-Hernández, S. Ulloa-Godinez, C. Velásquez and J. Arenas-Alatorre, *RSC Adv.*, **8**, 3108 (2018); https://doi.org/10.1039/C7RA12665D